Cover Page

Universiteit Leiden

The handle http://hdl.handle.net/1887/19114 holds various files of this Leiden University dissertation.

Author: Breij, Anastasia de
Title: Towards an explanation for the success of Acinetobacter baumannii in the human host
Issue Date: 2012-06-20
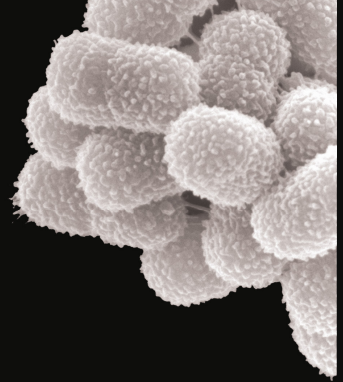
Chapter 6

Cryo electron tomographic analysis of membrane vesicle formation by *Acinetobacter baumannii* ATCC19606[T] at different growth stages

Roman Koning[1], Anna de Breij[2], Gert Oostergetel[3], Lenie Dijkshoorn[2], Peter Nibbering[2], Abraham Koster[1]

[1]Dept. of Molecular Cell Biology, Section Electron Microscopy, Leiden University Medical Center, Leiden, the Netherlands, [2]Dept. of Infectious Diseases, Leiden University Medical Center, Leiden, the Netherlands, [3]Faculty of Mathematics and Natural Sciences, Dept. of Electron Microscopy, University of Groningen, Groningen, the Netherlands.

Abstract

Acinetobacter baumannii is an important nosocomial pathogen responsible for colonization and infection of critically ill patients. The effect of the bacterium on the host follows from the interplay between virulence attributes of the micro-organism and the condition of the host. As some virulence attributes can be delivered to the host by membrane vesicles, this study aimed at characterization of the formation and morphology of membrane vesicles formed by *A. baumannii* ATCC19606[T] in vitro using cryo-electron tomography. Results revealed that different membrane vesicles were formed by *A. baumannii* during the various stages of its life cycle: (i) small outer membrane vesicles (OMVs; ±30 nm in diameter) formed at distal ends in the log-phase; (ii) larger OMVs (200-500 nm) formed at septa during cell division; (iii) inner and outer membrane vesicles (IOMVs; 100-300 nm) formed in the stationary phase, and (iv) OMVs with a rough surface formed in the late stationary phase. Exposure of *A. baumannii* to a sub-inhibitory concentration of the antibiotic ceftazidime resulted in filamentous forms that produced large numbers of OMVs. We argue that the different types of membrane vesicles formed during the various stages of the life cycle of *A. baumannii* play distinct roles in infection.

Introduction

Acinetobacter baumannii is a Gram-negative bacterium that can colonize and infect severely ill, hospitalized patients. Multidrug-resistant strains of *A. baumannii* have the propensity to spread among patients and numerous endemic and epidemic episodes caused by this species have been reported [13,32]. Although colonization is far more common than infection, severe *A. baumannii*-associated infections, including ventilator-associated pneumonia and catheter-related bloodstream infections, do occur [32]. Several virulence attributes are thought to play a role in *A. baumannii* infections, including its ability to adhere to and invade host cells [7,10,11,25], form a biofilm, induce host cell death [6], resist the killing actions of serum [20] and produce siderophores [15].

It has been reported that virulence factors of Gram-negative bacteria can be delivered to host cells by outer membrane vesicles (OMVs) [18,22,23]. OMVs are nanovesicles composed of outer membrane and periplasm components, such as phospholipids, proteins, and lipopolysaccharides (LPS) [1,26]. However, OMVs produced by a clinical *A. baumannii* isolate were found to contain not only proteins from the outer membrane, including the potent cytotoxic outer membrane protein A (OmpA), and the periplasm, but also components from the inner membrane and cytoplasm [23]. OmpA present on OMVs of *A. baumannii* can contribute directly to host cell death [18], indicating that OMVs from *A. baumannii* are an important vehicle to deliver bacterial effector molecules to host cells. Moreover, it has been suggested that *A. baumannii* release OMVs as a mechanism of horizontal gene transfer whereby carbapenem resistance genes can be delivered to surrounding *A. baumannii* isolates [34]. It is of note that these studies on the composition and function of OMVs of *A. baumannii* all used extensive purification methods for the isolation of OMVs, including (ultra)-filtration and centrifugation. A disadvantage of this isolation procedure could be the presence of inner membrane and cytoplasmic proteins in OMVs resulting from random capture by membrane fragments. Thus, these preparations may not represent the naturally occurring OMVs [22]. The aim of the present study was to characterize the formation and morphology of naturally formed membrane vesicles by *A. baumannii* ATCC19606[T] during the various stages of its life cycle using cryo electron tomography.

chapter 6

Material and Methods

Bacterial strain and culture conditions

A. baumannii ATCC19606[T] was used in the present study. Bacteria were preserved for prolonged periods in nutrient broth supplemented with 20% (v/v) glycerol at -80°C. For experiments, inocula from fresh overnight cultures on sheep blood agar plates were grown overnight in Luria Bertani (LB) medium at 37°C under shaking. One hundred microliters of the overnight culture were added to 15 ml of prewarmed LB medium in an Erlenmeyer flask and incubated at 37°C under vigorous shaking. Where indicated, bacteria were cultured for 2.5 h at 37°C under vigorous shaking in the presence of 4 mg/L ceftazidime (Sigma-Aldrich, Zwijndrecht, The Netherlands), i.e. below the MIC level of 16 mg/L of *A. baumannii* ATCC19606[T] [8].

Isolation of vesicles

Bacterial suspensions were cultured for 1, 2.5, 6, 20, and 48 h in LB medium at 37°C. Thereafter the bacteria were centrifuged for 10 min at 3,000 g and the supernatants were centrifuged for 1 h at 17,000 g to remove remaining cells and debris. Next, the pellets were resuspended in 1 to 2 ml phosphate buffered saline (PBS; pH 7.4) and these preparations were used for analysis by cryo electron microscopy.

Cryo electron microscopy

Cryo sample preparation

A few microliters of vesicle preparation were applied to glow-discharged lacey carbon EM grids. For cryo electron tomography, 5 or 10 nm protein A - gold particles were added as fiducial markers to the sample. Excess medium was automatically blotted onto Whatman no. 4 filter paper for 1 to 2 sec in a controlled environment operated at room temperature and 100% humidity. Subsequently, the specimen was vitrified by plunging into liquid ethane in a Vitrobot Mark IV (FEI Company, Eindhoven, The Netherlands). Samples were stored in liquid nitrogen until use. Grids were mounted in a Gatan 626 cryo holder (Gatan, Pleasanton, Germany) for cryo electron microscopy imaging.

Cryo electron microscopy

Cryo electron microscopy (cryo EM) was performed on several microscopes. For large scale automated data collection we used custom written software (unpublished) that was able to automatically scan and image large areas. These images were recorded on a Tecnai 12 electron microscope with a LaB$_6$ source and operated at 120 keV using a 4k x 4k Eagle camera (FEI Company). Cryo electron tomography (cryo ET) was performed on a Tecnai 20

FEG operated at 200 keV and a Tecnai G2 Polara operated at 300 keV (FEI Company). Images were recorded using Explore 3D software on a 2k x 2k camera mounted behind a GIF energy filter (Gatan) operated at a slit width of 20 eV. Cryo ETs of membrane vesicles were recorded with 2° tilt steps between -70° to +70° at a defocus of -5 micron, while tomograms of whole bacteria were recorded between -60° to +60° at a defocus between -6 and -8 micron and a magnification between 13,500 and 19,000 corresponding with a pixel size of 1.02 resp. 0.69 nm.

Image analysis and visualization
Tomographic tilt series were processed using IMOD version 3.9 [21]. Projection images were roughly aligned by cross-correlation and fine alignment was done using fiducial markers. The tomograms were reconstructed using weighted back-projection. Cryo electron tomograms were denoised using non-linear anisotropic diffusion. The number of OMVs and their size were measured using ImageJ [33]. Image segmentation and 3D surface rendering was performed using AMIRA version 5.2 (Visage Imaging, Berlin, Germany).

Results

Acinetobacter morphology
We investigated the general morphology of logarithmic phase *A. baumannii* ATCC19606[T] using cryo EM/ET (Figure 1). The bacteria did not form aggregates and readily attached to the carbon surface of the electron microscopy grid (Figure 1A). The size of (visibly classified) non-dividing bacteria was 1.54 ± 0.07 micron in length and 0.77 ± 0.04 micron in width (n=9). The bacterial outer membrane was smooth (Figure 1B) with occasional small ripples, predominantly at the distal ends. The distance between the outer and inner membrane layers was 33.4 ± 1.48 nm and the peptidoglycan layer measured about 7 ± 0.7 nm in width and was centered between the inner and outer membrane (Figure 1C, D).

The bacterial cell surface was covered by a ~150 nm thick layer with very low contrast and a radial appearance (data not shown). Also long filaments, bacterial fimbriae or pili, were extending from the surface of the bacteria as was observed earlier by others (11). The bacteria regularly contained 50-500 nm dark inclusions (Figure 1B) possibly containing phosphor, magnesium and potassium [3,16].
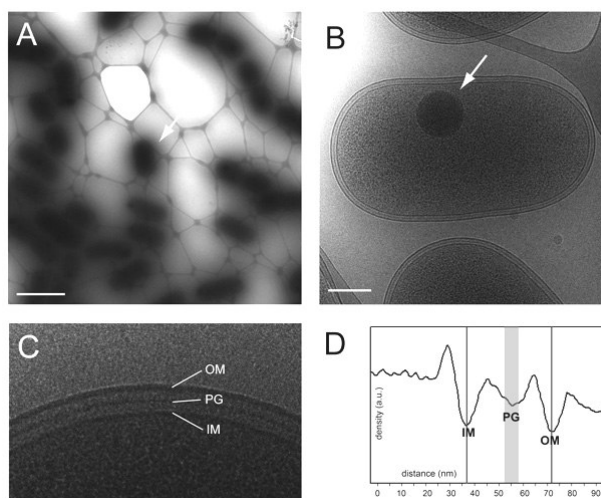
Figure 1. Cryo electron microscopic overview of *A. baumannii* ATCC19606[T] morphology and membrane structure. A*, A. baumannii* ATCC19606[T] (white arrow) on a lacey carbon support. B, Typical morphology of a single bacterium. In many cells a dark inclusion is present (white arrow). C, Detailed image of the bacterial membrane, showing the inner membrane (IM), the peptidoglycan layer (PG) and the outer membrane (OM). D, Density profile of the bacterial membrane showing the inner membrane, peptidoglycan and outer membrane. Scale bars are 2 µm (A) and 200 nm (B).

Formation and structure of membrane vesicles during logarithmic phase

In order to investigate whether the morphology and formation of membrane vesicles depends on the stage of the bacterial life cycle we imaged the vesicles from *A. baumannii* ATCC19606[T] cultured for 1 and 2.5 h (early and mid-logarithmic phase), 6 h (late logarithmic phase), and 20 and 48 h (early and late stationary phase, respectively).

Cryo ET recordings from 1 and 2.5 h cultured *A. baumannii* revealed the presence of ~30 nm vesicles budding off from the outer membrane (Figure 2B - G). These outer membrane vesicles (OMVs) were rarely observed possibly due to their small size and/or their limited occurrence. The formation of OMVs mainly occurred at the bacterial distal ends. At these sites we noted that the peptidoglycan layer was thickened and less dense, and the distance between inner and outer membrane was increased (Figure 2 A-F). In addition, large OMVs - typically 200-500 nm in diameter - were formed predominantly at sites of bacterial cell division (Figure 3A, B). Cryo ET on large OMVs showed that these vesicles lacked internal structures and displayed a smooth appearance (Figure 3C, D). These OMVs lacked fimbriae and the previously noted 150 nm thick low contrast layer that is present on the whole bacterium. Cryo electron microscopic images of OMV

formation indicated that these OMVs are connected to septa via a small outer membrane tubal structure (Figure 3B, E).
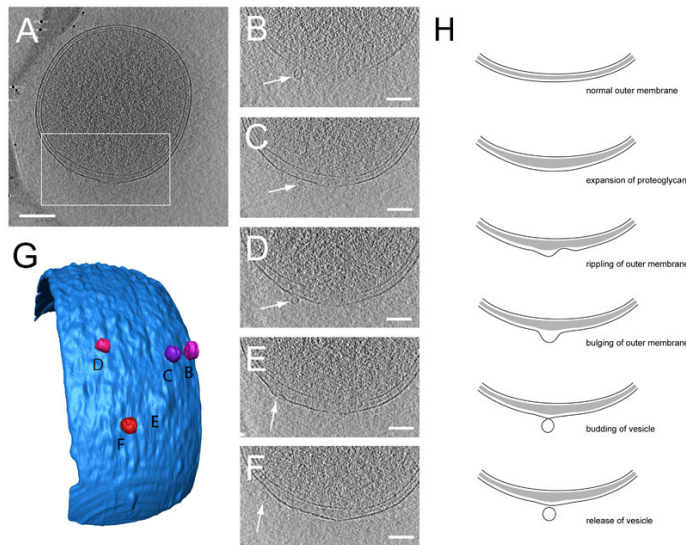
Figure 2. Formation of small outer membrane vesicles during logarithmic growth phase. A, Cryo electron tomographic slice of *A. baumannii*. B-F, Tomographic slices through the tomogram from the area that is outlined in (A) with white arrows indicating budding of outer membrane vesicles (OMVs). G, Surface representation of part of the bacterium that is outlined in (A) with colored in blue the bacterial outer membrane and in red to purple the formed OMVs. H, Schematic representation of the formation of small OMVs. Scale bars are 200 nm (A) and 100 nm (B to F).
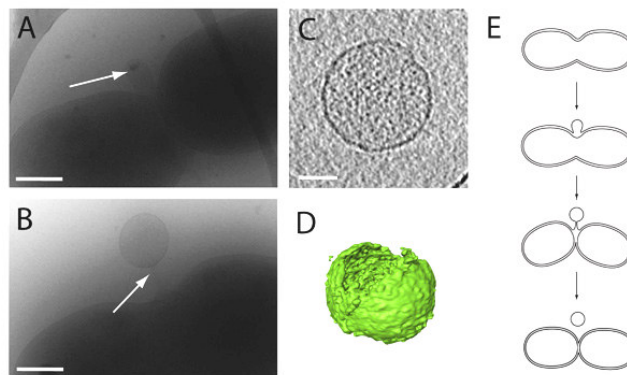
Figure 3. Formation of large outer membrane vesicles during logarithmic growth phase. A, Outer membrane vesicles (OMVs; white arrow) are often formed at or in the vicinity of bacterial septa during cell division. B, Sometimes OMVs are attached to the cell wall of dividing bacteria via a long tube (white arrow). C, Slice from a cryo electron tomogram through a large OMV reveal a smooth surface. D, 3D reconstruction of the tomogram in C. E, Schematic representation of the various stages of formation of large OMV at septa. Scale bars are 300 nm (A and B) and 50 nm (C).

Formation and structure of membrane vesicles during stationary phase

While in early (<6 h) bacterial cultures the number of vesicles was low, it dramatically increased during stationary phase (>6 h) cultures (Figure 4). The number of membrane vesicles did not linearly increase with the number of viable bacteria in the culture medium, suggesting that membrane vesicles are primarily formed from stationary bacteria and/or dying bacteria.
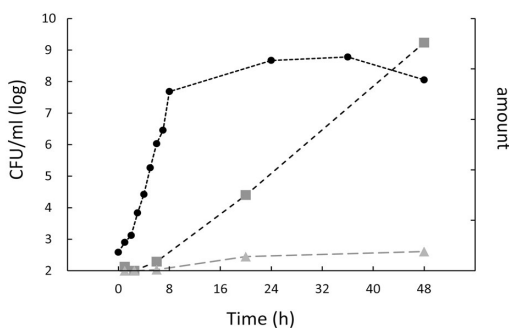
Figure 4. *A*. *baumannii* growth curve and membrane vesicle formation. The growth curve of *A. baumannii* ATCC19606[T] is plotted (round dots and black line) and the number of outer membrane vesicles (squares and dark grey striped line) and inner and outer membrane vesicles (triangles and light grey striped line) are plotted in time.

Also from cryo EM it appeared that the majority of membrane vesicles was formed by cellular degradation. While logarithmic phase *A. baumannii* exhibited a very regular shape, stationary bacteria often displayed anomalous shapes, such as bulges of the outer membrane (Figure 5A - C). It seemed that these deviating bacterial shapes are intermediates of bacterial fragmentation (Figure 5C, D) possibly associated with the process of bacterial cell death. Vesicles pinched off from dying bacteria, resulted in the formation of vesicles containing both inner and outer membranes (IOMV; Figure 5C, E - G, left panel), as demonstrated by tomographic reconstruction (Figure 5E, F). Probably IOMVs contain all components that are present in the periplasmic space and the cytoplasm (e.g. DNA). Almost all IOMVs contained a 150 nm low dense layer and fimbriae on their surface. These were occasionally observed in OMVs in stationary phase bacteria.

It appeared that in several IOMVs the inner membrane was dissociated or totally detached from the peptidoglycan layer, while this peptidoglycan layer remained associated with the outer membrane (compare Figure 5E and Figure 1C). Additionally, we observed intermediate structures with evidence of gradual breakdown of the inner membrane (Figure 5G) and secondary vesicle formation, i.e. membrane vesicle formation from IOMVs (Figure 5G, right panel). This breakdown of IOMVs and the formation of

membrane vesicles from IOMVs could explain the decrease in the relative numbers of IOMVs compared to the numbers of OMVs in later growth stages (Figure 4). The size of the membrane vesicles increased with the development from early logarithmic phase towards late stationary phase; OMVs being 72.3 ± 68.4 nm, while IOMVs were about 2 to 3 times larger (189 ± 115 nm).
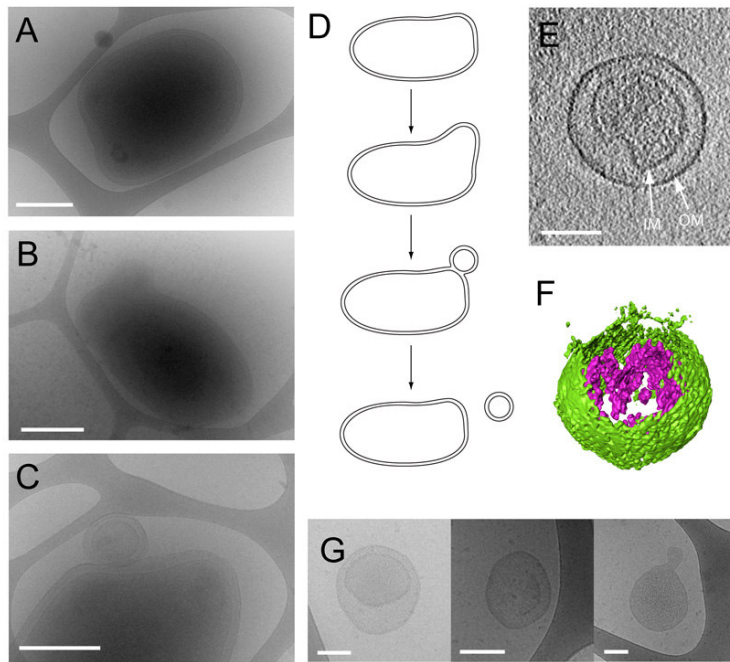
Figure 5. Formation of inner and outer membrane vesicles during late stationary phase. A, B, Bacteria deform and exhibit bulges that result in the (C) formation of membrane vesicles comprising both inner and outer membranes and peptidoglycan. D, Schematic representation of the stages of the formation of inner and outer membrane vesicles (IOMVs). E, Slice from a tomogram of an IOMV, with arrows showing the inner membrane (IM) and outer membrane (OM). F, 3D reconstruction of the tomogram in E, with in green the outer membrane and in purple the inner membrane. G, Once the IOMVs have been released from the bacteria they can have different shapes and the peptidoglycan and the inner membrane seem to degrade. Additionally, it appeared that MVs can arise from larger MVs. Scale bars are 300 nm (A, B and C) and 100 nm (E and G).

In *A. baumannii* cultures occasionally bacterial remnants were observed. In the most extreme case the bacterial remnants were transformed into a branched arrangement from which at the end OMVs were released (Figure 6A, B). These OMVs (Figure 6C - E) were rather uniform in size measuring roughly 75 nm. Cryo ET showed that the surface of

these vesicles had a rough appearance, being covered with small and large densities, most probable representing membrane (-associated) proteins (Figure 6E). On almost all these OMVs a large (10 nm) density was present (Figure 6D, E) that, judged by its shape and size, could be hemolysin (37). Large numbers of these rough OMVs were observed in the vicinity of bacterial remnants and given the surface area of an *A. baumannii* and the average radius of the OMVs, between 100 and 400 vesicles could be derived from a single bacterium.
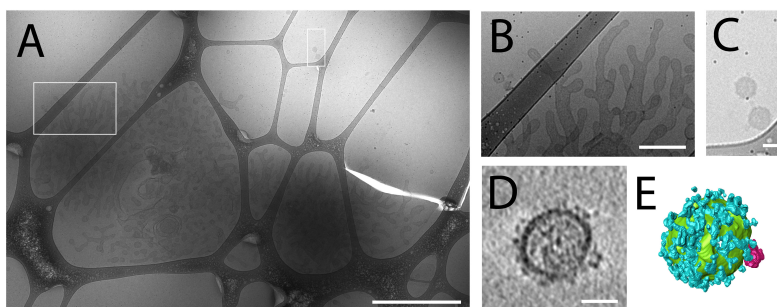
Figure 6. Formation of outer membrane vesicles from late stationary phase bacteria. A, outer membrane vesicles (OMVs) were formed form bacteria in their late stationary phase. B, From branching membrane structures OMVs are released (area from large white box in A). C, These OMVs are round and have a rough surface (area from large white box in A). D, Cryo electron tomography showed that these OMVs have many small densities on their surface and regularly contain a large cylindrical density. E, 3D reconstruction of the tomogram from D more clearly shows the rough surface and the densities that are suggestive for proteins (blue), the lipid membrane (green) and the large cylindrical protein complex (purple). Scale bars are 1 µm (A), 200 nm (B) and 50 nm (C) and 25 nm (D).

Effect of ceftazidime on vesicle formation

A sub-inhibitory concentration of the cephalosporin ceftazidime, which interferes with peptidoglycan synthesis, was added to *A. baumannii* cultures to investigate the effects of this antibiotic on the formation of OMVs. As expected in 2.5 h exposed cultures many filaments had been formed; in most extreme cases reaching lengths up to several tens of microns (Figure 7A). Membrane ruffling was observed along the whole outer membrane of ceftazidime-exposed bacteria instead of being localized solely to the distal ends of control bacteria. Additionally, deformations of the peptidoglycan layer and the outer membrane of antibiotic-exposed bacteria were observed frequently. In the presence of ceftazidime, membrane vesicle formation was more abundant than in the absence of the antibiotic. Especially at sites of potential septum formation (Figure 7B, C) and at distal ends (Figure 7D - F) membrane vesicle formation was more frequent than in control *A.*

baumannii. Cryo ET showed that these membrane vesicles often contained peptidoglycan at the inside and fimbriae and the low contrast layer on the outer surface (Figure 3G, H).
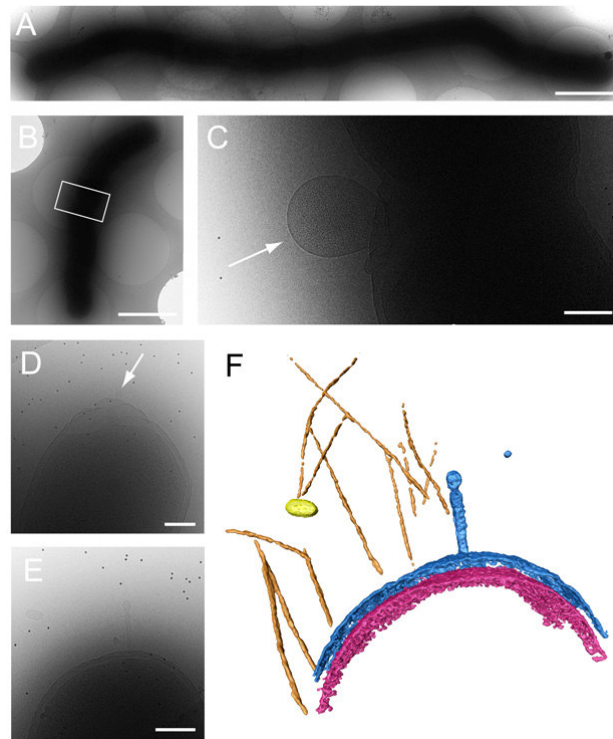
Figure 7. Formation of outer membrane vesicles by ceftazidime-treated bacteria. A, Ceftazidime inhibits bacterial division resulting in the formation of long bacterial structures. B, C, The formation of outer membrane vesicles (OMVs) was observed at potential sites of cell division with membrane roughing and peptidoglycan expansion (the white box in B depicts the position of C). D, At the bacterial distal ends, broadening of the peptidoglycan layer and formation of OMVs was regularly observed (white arrow). E, A large extension of the outer membrane. F, 3D reconstruction of the area in D shows OMVs (yellow) with attached fimbriae (orange), the formation of OMVs by bulging of the outer membrane (blue) and the inner bacterial membrane (purple). Scale bars are 2 µm (A and B), 200 nm (C to E).

Discussion

The main finding of the present study is that *A. baumannii* ATCC19606[T] forms morphologically diverse types of membrane vesicles during different stages of its life cycle. In exponentially growing bacterial cultures outer membrane vesicles (OMVs) were

formed mainly at distal ends of the bacteria and at septa of dividing cells. Stationary phase and dying bacteria released large numbers of vesicles, i.e. rough OMVs and inner and outer membrane vesicles (IOMVs), the latter were formed by partial fragmentation and budding off the cells. The timing of IOMV formation suggests that they are mainly derived from dying bacteria. These OMVs and IOMVs were abundant and it appeared that their surfaces were covered with low contrast material with a radial appearance, fimbriae and protein complexes. This is in accordance with the mass spectrometry measurements on purified membrane vesicles from *A. baumannii* [24]. It is conceivable that the biogenesis of membrane vesicle formation by *A. baumannii* in the present in vitro cultures may also occur in vivo. For example, Jin et al demonstrated that *A. baumannii* ATCC19606[T] secreted membrane vesicles during pneumonia in a mouse model of infection [18]. Others reported that *A. baumannii* present in alveolar macrophages in a patient with fatal *A. baumannii* pneumonia secreted multiple pleomorphic vesicles [28], suggesting the possibility of secretion of different types of vesicles during infection.

What are the functions of the various types of membrane vesicles in *A. baumannii* infection? It has been reported that pathogenic Gram-negative bacteria, including *A. baumannii*, deliver toxins and other virulence attributes to host cells via OMVs [2,17-19]. So far, proteomic studies on OMVs from *A. baumannii* including the ATCC19606[T] strain have indicated that inner membrane and cytosolic proteins as well as some virulence factors were present in these vesicles [19,23]. In addition, IOMVs of *A. baumannii* contain cytoplasmic material, including genetic material, and therefore they could be involved in gene transfer among bacteria. It should be noted that knowledge of the transfer of genetic material among clinical *A. baumannii* strains is still very limited. Together, further studies are clearly needed to identify the virulence attributes present in the various membrane vesicles formed by *A. baumannii* during its life cycle.

Other important findings pertain to the main mechanisms underlying the biogenesis of membrane vesicles in *A. baumannii*. Several genetic, biochemical, proteomic and microscopic observations have indicated that disruption of peptidoglycan synthesis genes and the removal of proteins that interconnect peptidoglycan-outer membrane interactions can lead to increased formation of OMVs [12,27]. Our cryo electron tomographic data showed that OMVs were formed primarily at sites where reorganization of peptidoglycan occurred, i.e. the peptidoglycan layer increased in thickness and was deformed, thus supporting the current models for OMV formation.

We found that sub-inhibitory concentrations of ceftazidime, which interferes with peptidoglycan synthesis by inhibiting the penicillin-binding-proteins (PBPs) in the cytoplasmic membrane of Gram-negative bacteria [9], resulted in filament formation, as described before [4]. These strands of non-dividing bacteria contain enhanced quantities

of LPS conferring the risk of delayed, higher release of LPS during treatment of infections [14]. Moreover, these sub-inhibitory concentrations of ceftazidime enhanced OMV production at distal and septal sites. It is conceivable that these OMVs carry LPS on their surface. Therefore, the possibility that inadequate dosing of antibiotics, such as penicillins and cephalosporins, has serious adverse effects in patients suffering from *A. baumannii* infection should be considered.

In this study we investigated both the formation and three-dimensional structure of naturally occurring membrane vesicles from *A. baumannii* using cryo electron tomography. To ensure optimal preservation of membrane vesicles from *A. baumannii* ATCC19606[T], we isolated the membrane vesicles from bacterial cultures by centrifugation steps only. This lenient isolation procedure limits rupture of cells and vesicles, stripping proteins from the surface and induction of vesicle fusion [22] resulting from harsh purification methods, that are regularly used in other studies. Furthermore, we employed cryo fixation of the samples using vitrification to preserve the membrane vesicles with high integrity. Cryo electron tomography has been used since this method is able to resolve cellular structures with high accuracy and resolution in three dimensions. In earlier investigations on the structure and formation of membrane vesicles either negative staining of purified MVs was employed or fixation, dehydration, staining and sectioning techniques were used [18,29-31,35]. In line with the above considerations, cryo electron tomography is increasingly used to study bacteria [5,36,38].

Our findings show that several types of membrane vesicles are formed by *A. baumannii* ATCC19606[T] during the different stages of the bacterial life cycle and we cannot exclude that these different types exert specific functions and have clinical significance.

Acknowledgements

chapter 6

References

1. Beveridge, T. J. 1999. Structures of gram-negative cell walls and their derived membrane vesicles. J.Bacteriol. 181:4725-4733.

2. Bomberger, J. M., D. P. Maceachran, B. A. Coutermarsh, S. Ye, G. A. O'Toole, and B. A. Stanton. 2009. Long-distance delivery of bacterial virulence factors by *Pseudomonas aeruginosa* outer membrane vesicles. PLoS.Pathog. 5:e1000382.

3. Bonting, C. F., G. J. Kortstee, and A. J. Zehnder. 1993. Properties of polyphosphatase of *Acinetobacter johnsonii* 210A. Antonie Van Leeuwenhoek 64:75-81.

4. Buijs, J., A. S. Dofferhoff, J. W. Mouton, J. H. Wagenvoort, and J. W. van der Meer. 2008. Concentration-dependency of beta-lactam-induced filament formation in Gram-negative bacteria. Clin.Microbiol.Infect. 14:344-349.

5. Butan, C., L. M. Hartnell, A. K. Fenton, D. Bliss, R. E. Sockett, S. Subramaniam, and J. L. Milne. 2011. Spiral architecture of the nucleoid in *Bdellovibrio bacteriovorus*. J.Bacteriol. 193:1341-1350.

6. Choi, C. H., E. Y. Lee, Y. C. Lee, T. I. Park, H. J. Kim, S. H. Hyun, S. A. Kim, S. K. Lee, and J. C. Lee. 2005. Outer membrane protein 38 of *Acinetobacter baumannii* localizes to the mitochondria and induces apoptosis of epithelial cells. Cell Microbiol. 7:1127-1138.

7. Choi, C. H., J. S. Lee, Y. C. Lee, T. I. Park, and J. C. Lee. 2008. *Acinetobacter baumannii* invades epithelial cells and outer membrane protein A mediates interactions with epithelial cells. BMC.Microbiol. 8:216.

8. Clark, R. B. 1996. Imipenem resistance among Acinetobacter baumannii: association with reduced expression of a 33-36 kDa outer membrane protein. J.Antimicrob.Chemother. 38:245-251.

9. Coulson, A. F. 1984. Microbiology: proteins that bind the beta-lactam antibiotics. Nature 309:668.

10. de Breij, A., L. Dijkshoorn, E. Lagendijk, J. van der Meer, A. Koster, G. Bloemberg, R. Wolterbeek, P. van den Broek, and P. Nibbering. 2010. Do biofilm formation and interactions with human cells explain the clinical success of *Acinetobacter baumannii*? PLoS.One. 5:e10732.

11. de Breij, A., J. Gaddy, J. van der Meer, R. Koning, A. Koster, P. van den Broek, L. Actis, P. Nibbering, and L. Dijkshoorn. 2009. CsuA/BABCDE-dependent pili are not involved in the adherence of *Acinetobacter baumannii* ATCC19606(T) to human airway epithelial cells and their inflammatory response. Res.Microbiol. 160:213-218.

12. Deatherage, B. L., J. C. Lara, T. Bergsbaken, S. L. Rassoulian Barrett, S. Lara, and B. T. Cookson. 2009. Biogenesis of bacterial membrane vesicles. Mol.Microbiol. 72:1395-1407.

13. Dijkshoorn, L., A. Nemec, and H. Seifert. 2007. An increasing threat in hospitals: multidrug-resistant *Acinetobacter baumannii*. Nat.Rev.Microbiol. 5:939-951.

14. Dofferhoff, A. S. M., J. Buys, and . 1996. The influence of antibiotic-induced filament formation on the release of endotoxin from Gram-negative bacteria. Journal of Endotoxin Research 3:187-194.

15. Dorsey, C. W., M. S. Beglin, and L. A. Actis. 2003. Detection and analysis of iron uptake components expressed by *Acinetobacter baumannii* clinical isolates. J.Clin.Microbiol. 41:4188-4193.

16. Hensgens, C. M., H. Santos, C. Zhang, W. H. Kruizinga, and T. A. Hansen. 1996. Electron-dense granules in Desulfovibrio gigas do not consist of inorganic triphosphate but of a glucose pentakis(diphosphate). Eur.J.Biochem. 242:327-331.

17. Horstman, A. L. and M. J. Kuehn. 2000. Enterotoxigenic *Escherichia coli* secretes active heat-labile enterotoxin via outer membrane vesicles. J.Biol.Chem. 275:12489-12496.

18. Jin, J. S., S. O. Kwon, D. C. Moon, M. Gurung, J. H. Lee, S. I. Kim, and J. C. Lee. 2011. *Acinetobacter baumannii* secretes cytotoxic outer membrane protein A via outer membrane vesicles. PLoS.One. 6:e17027.

19. Kesty, N. C., K. M. Mason, M. Reedy, S. E. Miller, and M. J. Kuehn. 2004. Enterotoxigenic *Escherichia coli* vesicles target toxin delivery into mammalian cells. EMBO J. 23:4538-4549. d

20. King, L. B., E. Swiatlo, A. Swiatlo, and L. S. McDaniel. 2009. Serum resistance and biofilm formation in clinical isolates of *Acinetobacter baumannii*. FEMS Immunol.Med.Microbiol. 55:414-421.

21. Kremer, J. R., D. N. Mastronarde, and J. R. McIntosh. 1996. Computer visualization of three-dimensional image data using IMOD. J.Struct.Biol. 116:71-76.

22. Kulp, A. and M. J. Kuehn. 2010. Biological functions and biogenesis of secreted bacterial outer membrane vesicles. Annu.Rev.Microbiol. 64:163-184.

23. Kwon, S. O., Y. S. Gho, J. C. Lee, and S. I. Kim. 2009. Proteome analysis of outer membrane vesicles from a clinical *Acinetobacter baumannii* isolate. FEMS Microbiol.Lett. 297:150-156.

24. Lee, E. Y., D. S. Choi, K. P. Kim, and Y. S. Gho. 2008. Proteomics in gram-negative bacterial outer membrane vesicles. Mass Spectrom.Rev. 27:535-555.

25. Lee, J. C., H. Koerten, P. van den Broek, H. Beekhuizen, R. Wolterbeek, M. van den Barselaar, T. van der Reijden, J. M. van der Meer, J. van de Gevel, and L. Dijkshoorn. 2006. Adherence of *Acinetobacter baumannii* strains to human bronchial epithelial cells. Res.Microbiol. 157:360-366.

26. Mashburn-Warren, L., R. J. McLean, and M. Whiteley. 2008. Gram-negative outer membrane vesicles: beyond the cell surface. Geobiology. 6:214-219.

27. McBroom, A. J., A. P. Johnson, S. Vemulapalli, and M. J. Kuehn. 2006. Outer membrane vesicle production by *Escherichia coli* is independent of membrane instability. J.Bacteriol. 188:5385-5392.

28. Mourtzinos, N., A. M. Schwartz, and J. M. Orenstein. 2007. Fatal *Acinetobacter baumanii* pneumonia diagnosed at autopsy in a patient with end-stage renal disease: a case report and review. Pathol Case Rev 12:122-125.

29. Muralinath, M., M. J. Kuehn, K. L. Roland, and R. Curtiss, III. 2011. Immunization with *Salmonella enterica* serovar Typhimurium-derived outer membrane vesicles delivering the pneumococcal protein PspA confers protection against challenge with *Streptococcus pneumoniae*. Infect.Immun. 79:887-894.

30. Palsdottir, H., J. P. Remis, C. Schaudinn, E. O'Toole, R. Lux, W. Shi, K. L. McDonald, J. W. Costerton, and M. Auer. 2009. Three-dimensional macromolecular organization of cryofixed *Myxococcus xanthus* biofilms as revealed by electron microscopic tomography. J.Bacteriol. 191:2077-2082.

31. Patrick, S., J. P. McKenna, S. O'Hagan, and E. Dermott. 1996. A comparison of the haemagglutinating and enzymic activities of Bacteroides fragilis whole cells and outer membrane vesicles. Microb.Pathog. 20:191-202.

32. Peleg, A. Y., H. Seifert, and D. L. Paterson. 2008. *Acinetobacter baumannii*: emergence of a successful pathogen. Clin.Microbiol.Rev. 21:538-582.

33. Rasband, W. S. ImageJ, U.S., National Institutes of Health, Bethesda, Maryland, USA, http://imagej.nih.gov/ij/.

34. Rumbo, C., E. Fernandez-Moreira, M. Merino, M. Poza, J. A. Mendez, N. C. Soares, A. Mosquera, F. Chaves, and G. Bou. 2011. Horizontal Transfer of the OXA-24 Carbapenemase Gene via Outer Membrane Vesicles: A New Mechanism of Dissemination of the Carbapenem Resistance Genes in *Acinetobacter baumannii*. Antimicrob.Agents Chemother. doi:AAC.00929-10.

35. Schooling, S. R. and T. J. Beveridge. 2006. Membrane vesicles: an overlooked component of the matrices of biofilms. J.Bacteriol. 188:5945-5957.

36. Shetty, A., S. Chen, E. I. Tocheva, G. J. Jensen, and W. J. Hickey. 2011. Nanopods: a new bacterial structure and mechanism for deployment of outer membrane vesicles. PLoS.One. 6:e20725.

37. Song, L., M. R. Hobaugh, C. Shustak, S. Cheley, H. Bayley, and J. E. Gouaux. 1996. Structure of staphylococcal alpha-hemolysin, a heptameric transmembrane pore. Science 274:1859-1866.

chapter 6

38. Tocheva, E. I., E. G. Matson, D. M. Morris, F. Moussavi, J. R. Leadbetter, and G. J. Jensen. 2011. Peptidoglycan Remodeling and Conversion of an Inner Membrane into an Outer Membrane during Sporulation. Cell 146:799-812.